Lasers in Manufacturing Conference 2025

Laser cutting of glass ribbon via melting at the draw.

Anatoli A. Abramov[a*1], Christopher Chilson[a], Mariia A. Lapina[b], Artemiy A. Shamkin[b], Boris N. Tsvetkov[b]

[a]*Corning, Sullivan Park Science & Technology Center, SP-AR-02-02, Corning, NY 14831, USA*
[b]*Corning Scientific Center, Salmisaarenaukio 1, 00180 Helsinki, Finland*

Abstract

In continuous glass manufacturing processes, such as fusion draw, it is essential to cut a glass ribbon into sheets without disruption of the glass flow. This is typically achieved through the use of mechanical or laser cutting apparatuses, which enable the separation process by cross-ribbon scoring followed by bend breaking. This study presents a method for on-draw cutting of hot glass ribbon through localized melting using an infra-red laser beam. Our findings demonstrate that cutting the ribbon, which is already formed but maintains temperature within the annealing range, allows full body ribbon separation through glass melting without generating excessive residual stress. Additionally, this laser-induced process results in the formation of a rounded edge, which might eliminate the need for further finishing in certain applications. An experimental platform, comprising the glass draw, and laser system developed along with a theoretical model of the process are presented.

Keywords: laser melting; glass; fusion draw

1. Introduction

Within continuous thin glass ribbon forming processes, such as fusion drawing or float glass production, it is necessary to partition a glass ribbon into sheets while preserving the uninterrupted flow of the material. This process is traditionally conducted using mechanical or laser cutting apparatuses, which enable separation through cross-ribbon scoring followed by bend breaking. This study introduces a novel method for on-draw cutting of hot glass ribbons through localized melting facilitated by mid-infrared laser radiation.

In general, glass melting, whether bulk or localized, is typically accompanied by the generation of residual stress within the glass volume or along its edges. This often necessitates a relatively lengthy annealing process and additional equipment to mitigate stress. However, if glass melting occurs when the glass body is heated to temperatures within the annealing range and maintained at that temperature, even for a brief period, the stress generated during the melting process can be significantly reduced compared to similar processes conducted at room temperature or at temperatures below the glass strain point.

The findings presented in this paper demonstrate that laser cutting the ribbon, which is already formed but still is within the annealing temperature range, enables complete separation via glass melting while minimizing the induction of residual stress. Furthermore, this laser-based technique results in the formation of a rounded edge, which may eliminate the need for additional finishing in certain applications.

In addition to the experimental demonstration of the separation process, a theoretical model was developed. This model, using a meshless method, not only provides a qualitative description of the mechanisms underlying the laser melting process but also predicts its dynamics and the behaviour of the glass surface within the softening-melting temperature range in the presence of high viscosity gradients. The model was validated through experimental data and aligns closely with key

* Corresponding author. Tel.: +1-607-974-9801
E-mail address: abramova@corning.com

observations. This validation enables the adaptation of the model for application to varying glass-laser source conditions, including glass thickness, composition, temperature, beam shape, power and others.

2. Experimental procedure

The proposed laser separation technique is based on the rapid and localized heating of the hot glass during the concluding phase of ribbon formation within the annealing zone. This localized heating is achieved through the use of a focused laser beam, which raises the temperature of the glass to its melting point, thereby enabling ribbon separation while simultaneously forming rounded edges. Furthermore, as the glass ribbon's temperature remains within the annealing range during the separation process, the residual stress induced by the laser melting is minimized.

To facilitate the separation of the glass ribbon, a round-shaped laser beam must be transformed into a narrow elliptical beam, with its major axis length exceeding the width of the ribbon. This configuration is conceptually illustrated in Figure 1a. The beam shaping process is accomplished using cylindrical optics, although beam scanning techniques may also be employed. The beam profile can take various forms, including Gaussian, flat-top, or bi-modal, which is generated through the superposition of two Gaussian beams. The beam delivery system is specifically designed to direct the laser beam toward the interior of the furnace via an open slot, providing direct access to the ribbon surface. An optical head equipped with beam-shaping optics is mounted on a motion system that tracks the movement of the ribbon and ensures that the laser beam remains fixed on the glass surface throughout each separation cycle. This arrangement is schematically depicted in Figure 1b. The ribbon melting process utilizes carbon dioxide laser radiation with a wavelength of 10.6 µm and a total power output of up to 500 W.

a) b)

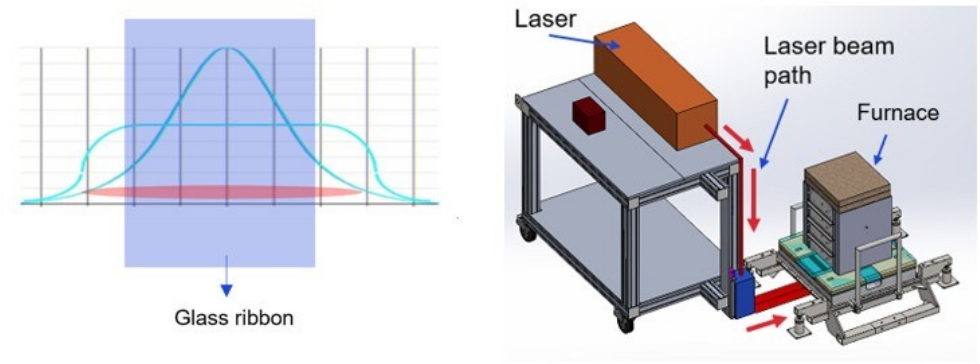

Fig. 1. (a) conceptual representation of laser heat profiles (Gaussian and flat-top) vs. glass ribbon; (b) schematics of the experimental set-up

Glass ribbon temperature is measured and controlled by an infrared camera. Typical temperature distribution is illustrated in Figure 2 (a, b), as an example, showing glass surface area, where annealing temperature is maintained, and where the laser beam can be applied for ribbon separation.

a) b)

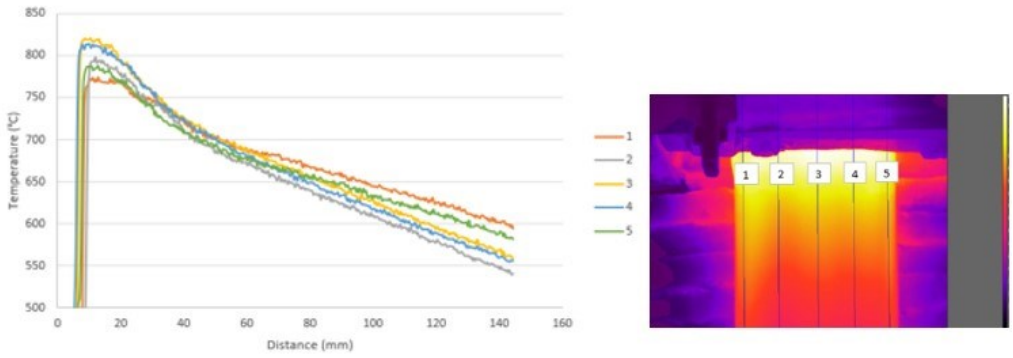

Fig. 2. (a) temperature drop along the ribbon; (b) thermal imaging of glass ribbon area subjected to laser irradiation

The thermal images in Figure 3 represent key stages of the laser separation process. Figure 3a depicts the temperature of the glass ribbon prior to the application of laser radiation. The maximum recorded background temperature within the controlled area in this case is about 855°C. The glass ribbon moves downward at a constant velocity, while the beam delivery system tracks the ribbon's movement to maintain synchronization with its velocity. Figure 3b illustrates the intermediate heating stage of the glass ribbon as it is subjected to the laser beam. During this phase, the maximum temperature within the beam-affected zone rapidly rises to 1386°C and continues to increase. Finally, Figure 3c captures the moment when the separation process begins at the right side of the glass ribbon. At this stage, the laser-induced melted zone propagates rapidly across the width of the ribbon, leading to complete separation of the glass body. Figure 4 shows both real (Figure 4a) and thermal (Figure 4b) images of the glass ribbon following the completion of the separation process. As the glass gradually cools down, its temperature remains within the annealing range for a short period of time.

a) b) c)

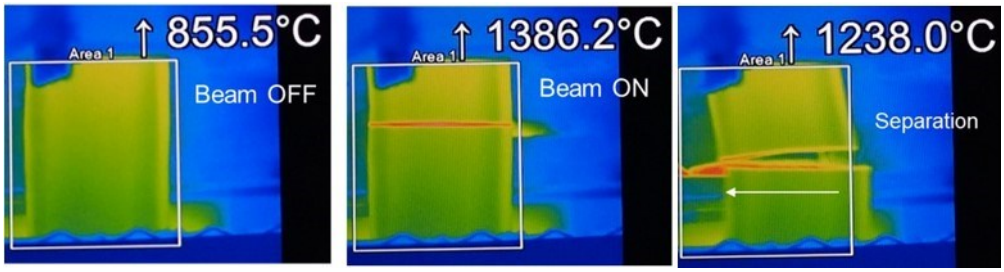

Fig. 3. (a) glass ribbon temperature prior to exposure to the laser beam; (b) ribbon temperature locally heated by the laser beam before the separation; (c) ribbon temperature at the end of the separation step

a) b)

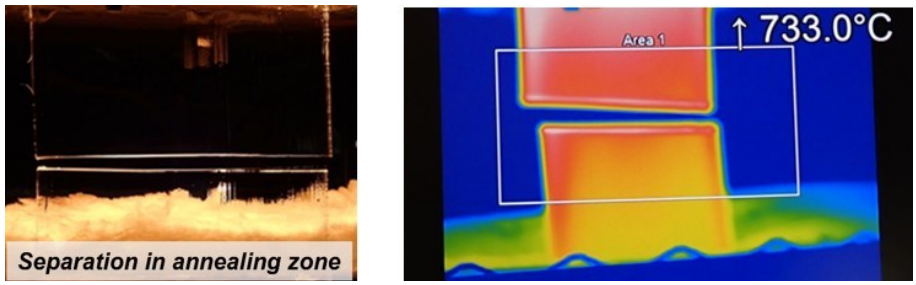

Fig. 4. (a) real image of the ribbon after laser separation in the annealing zone; (b) thermal image of the ribbon after laser separation in the annealing zone

During the separation step, as the glass is melted by the laser beam and subsequently cools, the newly formed edges of the glass adopt a rounded shape. This rounding is the result of the combined effects of draw tension, gravity, and the surface tension of the molten glass. The specific edge shape may vary across the ribbon and can differ depending on the glass ribbon's thickness. Figure 5 shows examples of the glass edge shapes formed as a result of laser melting for various glass thicknesses within the range from 0.075mm to 0.55mm. While the laser-melted edges might exhibit imperfections, they still achieve a reasonable level of quality and mechanical strength. These "finished-like" edges are suitable for certain applications, reducing or even eliminating the need for additional, costly post-processing steps.

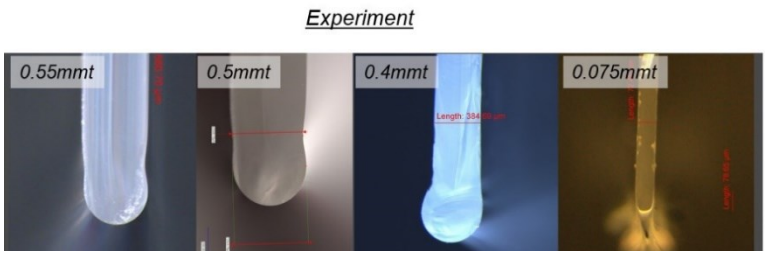

Fig. 5. Examples of cross-sections of glass edges formed as a result of laser melting for varying thicknesses within the range of 0.075-0.55mm

3. Modeling results and discussion

To investigate the mechanisms involved in the laser melting process and to better understand their roles in edge formation and process dynamics, a model based on a meshless method was developed. This model incorporates various factors to describe the process, including the heating of glass using concentrated laser power with different distribution profiles, glass absorption at a wavelength of 10.6µm, glass thickness, radiation losses, surface tension of the glass, high viscosity ratios, gravitational effect, and several other parameters. The conceptual framework of this approach is illustrated in Figure 6. The model was designed to simulate free surfaces of glass materials within the softening-to-melting temperature range, accounting for the high viscosity gradients induced by laser radiation. Experimental data obtained using the previously described equipment were utilized to validate the model's key assumptions and to calibrate its parameters.

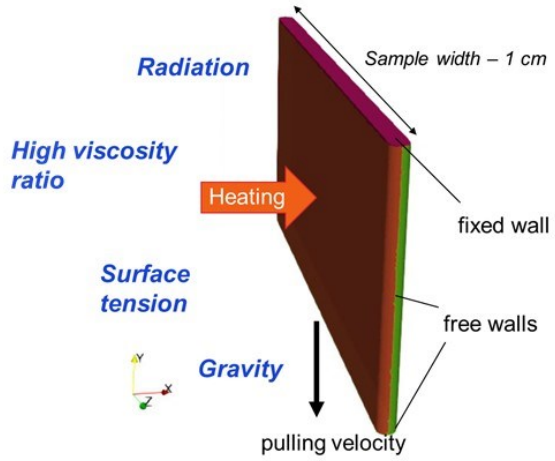

Fig. 6. Computational concept with highly localized heat flux

It was determined that laser melting cannot be accurately described using two-dimensional simulations. However, a three-dimensional model enables qualitative description of the process, aligning closely with key experimental observations. For instance, while 2D simulations demonstrate the thinning and separation of the glass layer under laser beam exposure, they fail to capture the formation of the rounded edge shape. This feature is represented in the 3D model, as illustrated in Figure 7.

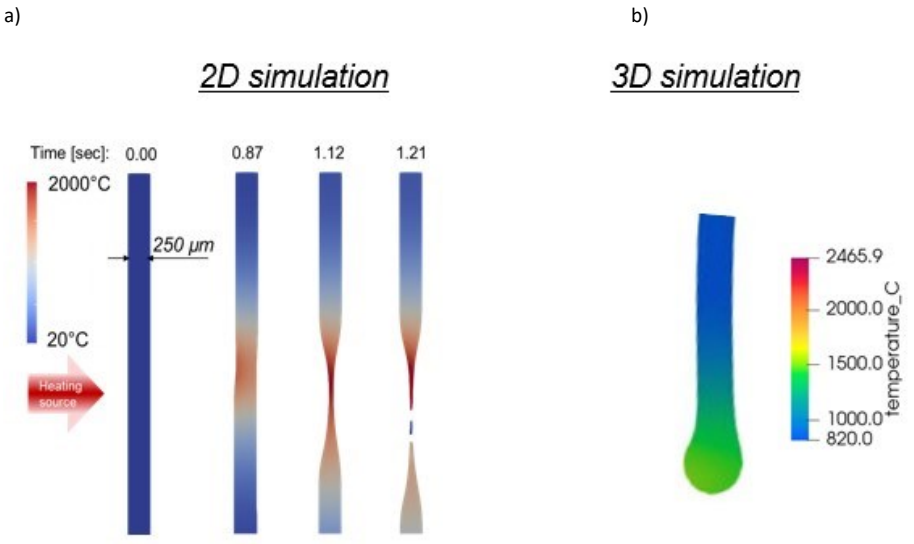

Fig. 7. (a) two-dimensional simulation depicting laser-induced separation and edge formation; (b) three-dimensional simulation illustrating the process with rounded edge formation

A comparison between experimental observations and modelling of ribbon separation revealed that the separation process does not necessarily initiate from the hottest zone. Instead, it is more likely to begin at the ribbon's side boundaries, potentially in regions with the minimum radius of curvature. This behaviour can be attributed to the asymmetric nature of the ribbon thickness variation, particularly in the beaded areas along the ribbon edges. As a result, the separation process typically initiates on one side of the ribbon. The corresponding simulation results, which depict the glass temperature distribution within the laser separation zone at specific moments after laser exposure begins, are shown in Figure 8. Figure 8a presents the case for a thin ribbon, while Figure 8b illustrates the results for a thicker ribbon as an example. Additionally, it was observed that a bi-modal heating distribution may offer advantages for separating ribbons with beads, especially in the case of thicker ribbons.

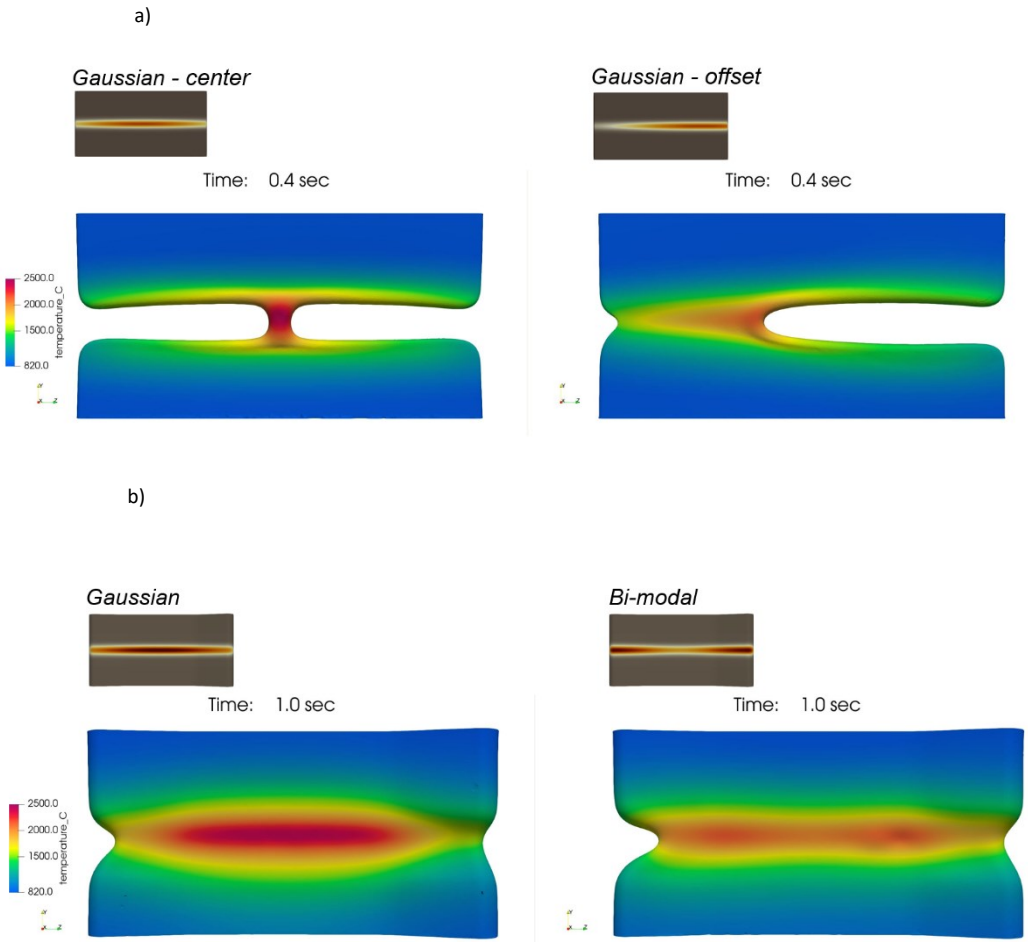

Fig. 8. (a) glass temperature distribution in the laser separation zone 0.4 seconds after the initiation of laser exposure for thinner glass; (b) glass temperature distribution in the laser separation zone 1.0 second after the initiation of laser exposure for thicker glass

Glass thickness and its variations across the ribbon have a significant impact on the dynamics of the separation process and serve as a limiting factor. This is primarily due to the fact that laser radiation at a wavelength of 10.6µm is highly absorbed by the glass skin layer, which has a depth of 5–15µm, while heat transfer through the glass thickness occurs relatively slowly. The most efficient and rapid separation was observed for ribbon thicknesses in the range of 0.075mm to 0.6mm, although thicker glass can also be separated. However, as demonstrated both experimentally and through simulations, the ribbon separation time increases substantially for thicker glass. Figure 9 illustrates the ribbon separation time for various glass thicknesses, providing a comparison between experimental data and modelling results.

Computations of separation time for various levels of laser power (e.g., -20%, +20%, +40%, etc.) and for varying power densities through adjustable beam widths reveal that increasing laser power reduces separation time, although the effect is limited. Similarly, narrowing the laser beam width, which increases power density, can slightly accelerate the separation process. The model was found to qualitatively predict the key process trends and ribbon behaviour, providing reasonably accurate estimates of the process parameters. The discrepancy observed between experimental and modelled values for

separation time, as shown in Figure 9, is primarily attributed to unaccounted thickness variations across actual ribbon samples and the assumed accuracy of glass characterization parameters at high temperatures within the model. This difference diminishes when flatter glass samples are tested. Further validation of the model through more precise comparisons with controlled experiments is feasible and would enable its adaptation to a wider range of glass-laser source configurations.

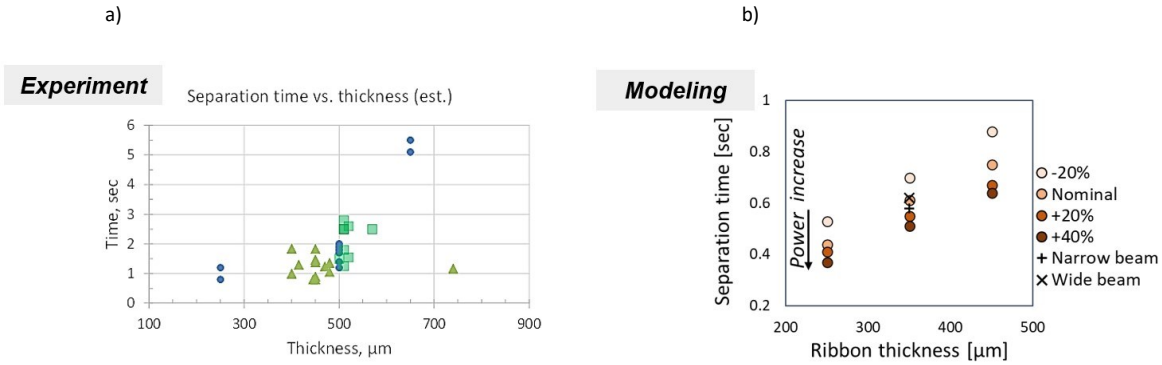

Fig. 9. (a) experimental separation time as a function of glass thickness; (b) calculated separation time for varying laser power levels and beam width as a function of glass thickness

4. Conclusion

A CO2 laser-based cutting technique facilitates full separation of glass ribbon during the draw process by rapidly melting the glass. This method produces "finished-like" edges with satisfactory mechanical quality and strength, significantly reducing the need for post-processing. The developed model, designed to simulate glass surface behaviour within the softening-to-melting temperature range and under conditions of high viscosity gradients, captures key experimental observations and qualitatively predicts the dynamics of glass separation.

Acknowledgements

The authors sincerely acknowledge the exceptional technical support provided by A. de Falussy, B. Marshall, J. Santarsiero, C. Schonher, R. Scouten, T. Sonner, and K. Waight.

References

Gusarov, A., Pavlov, M., Smurov, I., 2011. “Residual stresses at laser surface remelting and additive manufacturing”, Proceedings of the Sixth International WLT Conference on Lasers in Manufacturing. Munich, Germany. Physics Procedia 12, p.248.

Hildebrand, J., Hecht, K., Bliedtner J., Muller, H., 2011. “Laser beam polishing of quartz glass surfaces”, Proceedings of the Sixth International WLT Conference on Lasers in Manufacturing. Munich, Germany. Physics Procedia 12, p. 452.

Chen, K., Yang, T., Hong, R., Chiu, T., 2018. “Thermo-mechanical analysis of laser peeling of ultrathin glass for removing edge flaws in web processing applications”, Microsyst Technol 24, p.397.

Abramov, A., Black, M., Glaesemann, G., 2010. “Laser separation of chemically strengthened glass”, Proceedings of the Laser Assisted Net Shape Engineering 6. Erlangen, Germany. Physics Procedia 5, p. 285.